

# Chapter 5

## Space-time geometry of spiral galaxy halo

### 5.1 Introduction:

The astrophysical observations reveal that after the termination of luminous disk the expected Keplerian fall-off is absent in rotation curves (variation of angular velocity of test particles with distance from the galactic center) of spiral galaxies [181–185]. The frequency shift of the 21 cm HI emission line from neutral hydrogen cloud at large distances from the galactic center rotating in circular orbits allow to construct rotation curve of galaxies involving distances up to a few tens of kpc or even few hundreds of kpc in few cases. The observed flatness of galactic rotation curves implies that either the Galaxy contains far more matter than contributed by the luminous matters such as stars, planets and the gas or the laws of gravity is different at large distances. The velocity dispersion of galaxies in the galactic clusters [186, 187], gravitational lensing by galaxies [187–192, 192] also support the existence of invisible matter which is commonly referred as dark matter.

The dark matter hypothesis has also received support from the cosmological observations. The  $\Lambda$ CDM model, where  $\Lambda$  is the cosmological constant and CDM stands for cold dark matter, fits the cosmological observations well and is quite successful in describing the formation and evolution of the large scale structure in the Universe (see for instance [193, 194]). In cosmology the cold dark matter hypothesis draws from two phenomena - inflation and big-bang nucleosynthesis.

The inflationary idea suggests that the Universe is nearly flat with matter density equals to critical density which receives support from the observed anisotropy features in the cosmic microwave background radiation (CMBR) [195]. The baryon density inferred from nucleosynthesis suggests that ordinary matter can contribute at most 15% of the critical density [196]. Hence if the inflationary picture is correct, then most of the matter in the Universe must be nonbaryonic. The  $\Lambda$ CDM model interprets that the gravitational attraction of cold dark matters leads to formation of cosmic structures and it also plays important role in holding the structures together.

The space time geometry of galactic halo in presence of dark matter is a very relevant issue. Besides study of the effects of gravitational interactions in the galactic halo region it also offers possibility of cross-verification of existence of dark matter itself through different local gravitational phenomena such as gravitational lensing, gravitational time delay [137], time advancement [127, 140, 197] etc. A naive Newtonian analysis suggests that the tangential velocity ( $v_\varphi$ ) of rotation  $\beta_\varphi = \sqrt{\frac{GM}{c^2 r}}$ , where  $\beta_\varphi = v_\varphi/c$ ,  $c$  is the speed of light,  $G$  is the gravitational constant(CMBR),  $M$  is the total mass inside the radius  $r$  of the galaxy and  $r$  is the distance from the galactic center. The observed flatness of galactic rotation curves implies that  $M$  is a function of  $r$  that increases linearly with  $r$ . In Newtonian analysis the galactic gravitational potential is expressed accordingly as  $\frac{GM(r)}{r}$ . Newtonian treatment is, however, inadequate to describe the true and complete gravitational field of galactic halo as required for gravitational lensing and similar other local gravitational phenomena.

Several attempts were made to model dark matter halos in the general relativistic framework. In the Newtonian approach gravitational field is solely represented by gravitational potential. In Newtonian concept the matter density solely plays the role of generation of the gravitational potential which can be completely determined by the observed rotation curve in the galactic halo region. In contrast, even in the spherically symmetric situation general relativistic analysis requires knowledge of two metric coefficients ( $g_{tt}$  and  $g_{rr}$ ), to completely describe the gravitational field of galactic halo. One of the underlying reasons for such a difference is that in the general relativistic framework pressure also contributes to gravitational field unlike in the Newtonian approach. While the  $g_{tt}$  can be obtained from the features of rotation curve, additional input about the equation of state of dark matter is required to determine  $g_{rr}$ . Applying general relativistic prescription and

invoking observed flat rotation curve feature, several researchers proposed space time geometry of galactic halo considering dark matter as minimally coupled scalar field with potential [150, 152, 198, 199], as scalar field in Brans-Dicke theory [200], as perfect fluid [201], as quintessential matter [202], in Brane world scenario [203] etc. The metric coefficient  $g_{rr}$  in the mentioned works [150, 152, 198–203] are different, depending on the choice of the equation of state of dark matter, but  $g_{tt}$  is the same in all the cases, proportional to  $r^{\beta_\phi^2}$  as obtained from the flat rotation curve feature. In all the stated works, a non-zero pressure of dark matter particles was considered for deriving the gravitational field.

Under the context the objective of this chapter is to explore for a general relativistic solution of space time geometry of galactic halo in presence of CDM which will be consistent with the observed flatness of rotation curve and will respect the basic principles of general relativity. Note that our objective is not to model the dark matter of galaxy, rather we shall derive the space time metric in the galactic halo region taking the observed feature of galactic rotation curve as an input and assuming the presence of cold dark matter in galaxy. The gravitational lensing observations provide another compelling evidence for existence of dark matter in galactic halo. We shall study the gravitational lensing due to the space time metric of galactic halo as derived in this chapter.

The organization of the chapter is as the following. In the next section (5.2) we shall evaluate the gravitational potential at galactic halo exploiting observed flat rotation curve feature and considering the presence of cold dark matter. We shall discuss other relevant issues like stability of circular geodesics in the same section. In section 5.3 we shall study gravitational lensing due to the derived space time metric. We shall discuss our results in section 5.4 and finally conclude in the same section.

## **5.2 Galactic potential in presence of cold dark matter invoking observed flat rotation curve feature:**

In Newtonian gravity the tangential velocity of a test particle in circular orbits around the central mass distribution is obtained simply by equating the centripetal

acceleration with the gravitational acceleration due to central mass that leads to  $v_\varphi = \sqrt{\frac{GM}{r}}$ . The determination of tangential velocity in GR framework is slightly complex. Assuming that the galactic halo is spherically symmetric, the general static space time metric of the halo can be written in curvature coordinates as [204]

$$ds^2 = -e^{2\lambda(r)}dt^2 + \frac{dr^2}{1 - \frac{2m(r)}{r}} + r^2(d\theta^2 + \sin^2\theta d\phi^2), \quad (5.1)$$

where  $\lambda(r)$  and  $m(r)$  are functions of  $r$  only. We are expressing quantities in natural units i.e.  $c$  and  $G$  are taken as 1. The function  $\lambda(r)$  is known as the “potential” and  $m(r)$  is the shape function which essentially reflects the effective gravitational mass. Assuming that test particles move on the equatorial plane ( $\theta = \pi/2$ ) the tangential velocity of a non-relativistic test particle in a circular orbit can be obtained from the study of geodesics for the above space-time metric which is given by [198, 199, 201]

$$\beta_\varphi^2 = r\lambda'(r) \quad (5.2)$$

where prime denotes the derivative with respect to  $r$ . Since observations suggests that  $\beta_\varphi$  is nearly constant at large galactic distances, the above equation immediately gives at halo region  $e^{2\lambda(r)} \propto r^{2\beta_\varphi^2}$ . This form of  $g_{tt}$  is adopted in the several previous works [150, 152, 198–203] for galactic halo.

Here we look for a form of  $g_{tt}$  that can be recast as perturbation of Minkowski metric as expected in the weak gravitational field regime. Since the gravitational field is weak in the halo region we consider the metric in the halo region can be written as  $g_{\mu\nu} = \eta_{\mu\nu} + h_{\mu\nu}$ , where  $h_{\mu\nu}$  is the small perturbation over the Minkowski metric  $\eta_{\mu\nu}$ . Accordingly we write  $g_{tt}$  of equation (5.1) as

$$e^{2\lambda(r)} = 1 - \frac{2M_B}{r} + f(r), \quad (5.3)$$

where  $f(r)(\equiv h_{tt})$  is a function of  $r$  that arises due to presence of dark matter and  $M_B$  is the total baryonic matter of the galaxy within radius  $r$ . The observations suggest that after the galactic bulge the density of baryonic matter is very small and  $M_B$  may be taken as a constant. When  $r$  is small,  $f(r)$  is smaller than

$\frac{2M_B}{r}$  and vice versa for large  $r$ . In the galactic halo region we may approximate  $e^{2\lambda(r)} \simeq 1 + f(r)$ . Since the magnitude of  $\beta_\phi^2$  is very small we shall keep only the leading order terms in  $\beta_\phi^2$  in the solution of halo metric ignoring higher order terms. When flat rotation curve feature is invoked, the equation (5.2) leads to the following solution

$$f(r) \simeq 2\beta_\phi^2 \ln r + C1 \quad (5.4)$$

where  $C1$  is an integration constant which may be fixed from the boundary conditions. Note that the above solution does not necessarily require the presence of dark matter; it follows from the observed flatness feature of galactic rotation curve at outskirts of spiral galaxies. At present one cannot rule out the possibility that some modification of general relativity could be the origin of the logarithmic form in the potential.

### 5.2.1 Space time geometry of halo for cold dark matter

For complete understanding of space-time geometry in the halo region the knowledge about  $g_{rr}$  is also required. Additional input in the form of dark matter equation of state is needed to determine  $g_{rr}$ . The nature of dark matter is an unanswered issue of contemporary astrophysics. The only information available about dark matter is that it has not shown any interaction with the baryonic matter except the gravitational interaction.

Numerical simulations of structure growth suggests that dominant part of the dark matter in the universe is preferably "cold" i.e. velocity of dominant part of the dark matter particles is much less than the speed of light. Though the  $\Lambda$ CDM model receives an indisputable success on large scales, validity of the CDM scenario on galactic scales has been questioned in several works. It is found from N-body numerical simulations that CDM halos and sub-halos should have a high density (cuspy) profile at the centre [205–207]. The CDM model also gives overabundance of dwarf galaxies in the Milky Way and other similar galaxies/local groups against the observations, which is the so called missing satellites problem [208–210]. There are other issues like the so called too-big-to-fail problem [211, 212]. However, recent studies claim that except the core-cusp problem, other discrepancies between observations and CDM based simulations are removed when baryonic effects are properly taken into consideration in the simulation [213]. The warm cold matter

(WDM) has been proposed in the literature as an alternative to CDM [214, 215] but the WDM model also shares the core-cusp problem in galactic scale [216]. Besides, high redshift Lyman- $\alpha$  forest data disfavors the WDM model [217]. There is also a possibility that the core-cusp problem originated due to our poor understanding of galaxy formation or due to improper underlying assumptions in the N-body simulations [218, 219]. Theoretically weakly-interacting massive particles is the most attractive dark-matter candidates from particle physics point of view which falls under the cold dark matter category. Considering all the aspects and the overall performance over large scales and galactic scales CDM model still remains the most favored dark matter model. We shall, therefore, derive  $g_{rr}$  from Einstein field equation considering that the pressure of dark matter is negligibly small i.e. considering essentially the energy momentum tensor of cold dark matter.

Considering that the dark matter as a fluid with energy density  $\rho(r)$ , radial pressure  $p_r(r)$ , and tangential pressure  $p_T(r)$ , the Einstein field equations for dark matter halo read (we shall take  $c = 1$  through out the manuscript) :

$$\frac{2m'(r)}{r^2} = 8\pi\rho \quad (5.5)$$

$$\frac{2}{r^2} \left[ r\lambda'(r) \left( 1 - \frac{2m(r)}{r} \right) - \frac{m(r)}{r} \right] = 8\pi p_r \quad (5.6)$$

$$\begin{aligned} & \left( 1 - \frac{2m(r)}{r} \right) \left( \lambda''(r) + \lambda'^2(r) + \frac{\lambda'(r)}{r} \right) \\ & - \frac{1}{r^3} [m'(r) - m(r)] [1 + r\lambda'(r)] = 8\pi p_T. \end{aligned} \quad (5.7)$$

Now we consider the followings: In the galactic halo region  $m(r) \gg M_B$ . For cold dark matter  $p_r = p_T = 0$ . Inserting the flat rotation curve led metric coefficient  $e^\lambda$  i.e. expression given in equation (5.4) in equations (5.6) and (5.7) we get to the accuracy of  $\beta_\varphi^2$

$$m(r) \simeq \beta_\varphi^2 r \quad (5.8)$$

The above equation together with equation (5.4) completely specify the halo space time geometry.

### 5.2.2 Matching with the exterior Schwarzschild space time

In general relativity the Schwarzschild metric is the unique static vacuum solution and thus represents the exterior space time of galaxies with mass parameter equals to total mass  $M_T$  content of the galaxy. The solution derived above must match the exterior Schwarzschild metric at galactic boundary. We consider the junction conditions given by given by O'Brien and Synge [220, 221] i.e. the metric tensor and all the first order partial derivatives  $\frac{\partial g_{\mu\nu}}{\partial x^\zeta}$  except possibly  $\frac{\partial g_{rr}}{\partial r}$  should be continuous at the junction. Note that a solution satisfying the junction conditions of O'Brien and Synge always can be transformed to one satisfying the conditions of Lichnerowicz [222] and vice versa [223, 224].

The matching of metric tensor  $g_{tt}$ ,  $g_{ii}$  (i=1,3) and  $\frac{\partial g_{tt}}{\partial r}$  at galactic boundary ( $r = R_G$ , where  $R_G$  is the radius of the galaxy) consistently suggest that  $C1 = 2\beta_\varphi^2(1 - \ln R_G)$  and

$$M_T = M_B + \beta_\varphi^2 R_G. \quad (5.9)$$

The matching of  $\frac{\partial g_{rr}}{\partial r}$  at galactic boundary can be achieved by a coordinate transformation as demonstrated in [224] for general class of solutions.

### 5.2.3 The space time geometry of galactic halo

Thus finally the space-time metric of galactic halo(CMBR) appears as

$$\begin{aligned} ds^2 = & - \left( 1 - 2\beta_\varphi^2 - \frac{2M_B}{r} + 2\beta_\varphi^2 \ln(r/R_G) \right) dt^2 \\ & + \frac{dr^2}{1 - 2\beta_\varphi^2 - \frac{2M_B}{r}} + r^2(d\theta^2 + \sin^2\theta d\phi^2). \end{aligned} \quad (5.10)$$

For the metric given in equation (5.1) circular orbits will exist when  $0 < r\lambda' < 1$  which is indeed the case for the solution given in equation (5.10). The time-like circular geodesics has to be stable for a viable space time geometry of the galactic halo. The condition for stable circular orbit for the metric given in equation (5.1)

is [225]

$$3\lambda' + r\lambda'' > 2r\lambda'^2 \quad (5.11)$$

As  $\beta < 1$ , the above condition satisfies for the derived metric.

Inserting the solution of  $m(r)$  in equation (5.5), the density of dark matter is readily obtained as

$$\rho \simeq \frac{1}{4\pi} \frac{\beta_\varphi^2}{r^2} \quad (5.12)$$

At least in the outer parts of galaxies dark matter has a mass density profile closely resembling that of an isothermal sphere.

The total gravitational energy  $E_G$  between two fixed radii, say  $r_i$  and  $r_o$  in the halo region can be estimated for the metric (5.10) following [226] which is given by

$$E_G = M_{DM} - E_M = 4\pi \int_{r_i}^{r_o} \left[ 1 - \left( 1 - \frac{2m(r)}{r} \right)^{-1/2} \right] \rho r^2 dr \quad (5.13)$$

where  $M_{DM}$  is the dark matter mass (we have ignored the contribution of luminous matter) which is given by

$$M_{DM} = 4\pi \int_{r_i}^{r_o} \rho r^2 dr \simeq \beta_\varphi^2 (r_o - r_i) \quad (5.14)$$

The gravitational energy  $E_G$  is, therefore, given by

$$E_G \simeq -\beta_\varphi^4 (r_o - r_i) \quad (5.15)$$

which is negative as expected owing to positive  $\rho$  and the gravitational field of the halo is, thereby, attractive.



### 5.3 Gravitational lensing due to gravitational field of galactic halo

It is often argued that combined observations of galaxy rotation curves and gravitational lensing can provide better insight of the gravitational field of the galactic halo [227, 228]. In [228] it was shown that the form of gravitational potential extracted from rotation curve  $\lambda_{RC}(r)$  and lensing observations  $\lambda_{Lens}(r)$  are not the same in general:

$$\begin{aligned}\lambda_{RC}(r) &= \lambda(r), \\ \lambda_{Lens}(r) &= \frac{1}{2}\lambda(r) + \frac{1}{2} \int \frac{m(r)}{r^2} dr\end{aligned}\tag{5.16}$$

For the halo metric given in (5.10),  $\lambda_{RC}(r) = \lambda_{Lens}(r) = \lambda(r)$  owing to pressure less fluid.

In gravitational lensing scenarios when photon trajectories are outside the galaxy, which is the case in most of the observations involving external galaxies/galaxy clusters as lens, the gravitational deflection will be that due to Schwarzschild geometry with total mass as given by equation (5.9). In such cases the gravitational lensing phenomenon can provide information about the total mass of the galaxy, check the validity of equation (5.9) and thereby the halo metric. When the null geodesics are through galactic halo the lensing phenomenon may additionally probe the space time geometry of halo.

When source and observer are at large distance away compare to the distance of closest approach ( $r_o$ ), for the metric given in equation (5.1) the gravitational bending angle over the journey from  $r_o$  to infinity may be written as

$$\phi(r_o) - \phi(r_\infty) = \int_{r_o}^{\infty} \frac{dr \sqrt{\left(1 - \frac{2m(r)}{r}\right)^{-1}}}{r \sqrt{\left[\frac{r^2}{r_o^2} \left(\frac{e^{2\lambda(r_o)}}{e^{2\lambda(r)}} - 1\right) - 1\right]}}\tag{5.17}$$

For the halo metric given in equation (5.10), the total bending angle to the leading order in  $m/r$  and  $\beta_\varphi$  will be

$$\alpha \simeq \frac{4M_B}{r_o} + 2\beta_\varphi^2 \pi . \quad (5.18)$$

Therefore, the deflection angle will be enhanced by a constant factor  $2\beta_\varphi^2$  over the Schwarzschild value for light trajectory from source to observer. Note that the conventional dark matter model (Newtonian) also gives constant bending angle when distance of closest approach of photon trajectories are within the galaxy. Usually Schwarzschild deflection angle is employed to interpret lensing observations. The Schwarzschild deflection angle ( $\frac{4M(r)}{r_o}$ ) becomes a constant when (dark matter) mass increases linearly with halo radius. Here a point to be noted: the expression for Schwarzschild deflection angle is evaluated under the assumption that mass parameter  $M_T$  is a constant, independent of radial coordinate. So application of Schwarzschild deflection angle for dark matter radial dependent mass is not proper if distance of closest approach is within the galaxy.

The angular position of the images ( $\zeta$ ) can be obtained from the lens equation in the weak lensing scenario is given by [229]

$$\zeta = \beta + \frac{d_{ls}}{d_{os}} \alpha \quad (5.19)$$

where  $\beta$  denotes the angular source position,  $d_{ls}$  and  $d_{os}$  are the distances between lens and source and observer and source respectively. The image positions can be obtained from the above equation after inserting the expression for bending angle either from equation (5.18) or the Schwarzschild deflection angle depending on whether the distance of closest approach is inside or outside the galaxy.

If mass of baryonic matter in galaxy is known independently by some other method such as through photometry, the prediction of halo space time metric can be tested observationally through lensing observations.

The expression of image position in weak field Schwarzschild lensing is given by

$$\zeta_\pm = \frac{1}{2} \left( \beta \pm \sqrt{4\alpha_0 + \beta^2} \right) \quad (5.20)$$

where the indices  $\pm$  denote the parities of the images, and

$$\alpha_0 \equiv \sqrt{\frac{d_{ls}}{d_{ol}d_{os}}} 4M_T . \quad (5.21)$$

An important question at this stage is that whether the halo space time geometry can be verified from observational lensing data or not. Since the presence of dark matter is clearly revealed in galaxy clusters, here we have considered the case of gravitational lensing by cluster Abell 370 in which the ‘giant luminous arcs’ were first observed [172, 173]. Our objective is to first estimate  $M_T$  from the lensing observation and subsequently we shall compare the so evaluated  $M_T$  with that given by equation (5.9).

Galaxy clusters have complex matter distributions in general and cannot be considered to be either point masses or spherically symmetric mass distribution. However, a spherically symmetric lens model can be employed as a first approximation to extract the same order of magnitude results as the more realistic case analyzing the large arcs that are observed in clusters [177, 178]. We have considered the luminous arc, A0, which has a radius of curvature of about  $25''$  [176] and treat the arc as an Einstein ring [174, 176]. The observed redshift ( $z_s$ ) of A0 is 0.724 which gives the distance of the background galaxy and the lens distance is obtained from the redshift 0.374 of Abell 370. A concordance cosmological model of  $(\Omega_m, \Omega_\Lambda, \Omega_k) = (0.3; 0.7; 0)$  is applied for distance estimation from redshifts of lens and source. Our estimated total mass from lensing observations is given in Table 5.1.

The estimated mass of the luminous matter in Abell 370 from photometric measurement is found at least two orders smaller than the total mass of Abell 370 [176]. We use  $\beta_\phi$  as velocity of dispersion for Abell 370 which is  $1367 \text{ km s}^{-1}$  [176, 230]. The radius of the galaxy is an unknown parameter which we have taken equal to Einstein radius as a first approximation i.e. about 200 kpc which is consistent with the findings from Hubble imaging observations [180]. The total mass obtained from equation (5.9) is also given in Table 5.1. We find that the mass obtained from equation (5.9) agrees reasonably well with the lensing observations.

Interestingly the lensing results also can be utilized to check the validity of baryonic Tully-Fisher relation [231]. Tully & Fisher first demonstrated that an empirical power law relation exists between luminosity and rotation velocity of galaxies [232]. However, the optical Tully-Fisher relation exhibits a break; the power law index differs for fainter and brighter galaxies [231]. The rotational velocity of galaxies is found to exhibit a single power law relation with total baryonic disk mass, which is

TABLE 5.1: Estimated baryonic mass of Abell 370

Object	$z_l$	$z_s$	$r_E$ in arcsecs	$M_T/M_\odot \times 10^{-11}$ from lensing data	$M_B/M_\odot \times 10^{-11}$ from equation (5.9)
<i>Abel370</i>	0.374	0.724	25	923.06	873.3

the sum of stellar mass and gas mass of galaxy, instead of luminosity. The baryonic Tully-Fisher relation is given by  $M_B \propto \beta_\phi^4$ . We would like to replace rotational velocity by baryonic mass. A sample of rotational velocity data for galaxies with large variation in mass are shown in Table 2 which are taken from [233–235]. The variation of  $\beta_\phi^4$  with  $M_B$  from the observed data is shown in Fig. (5.1). Expressing the rotational velocity as  $\beta_\phi^4 = a_{tf}^2 M_B$  where  $a_{tf}^2$  is a proportionality constant, we get by the least square fitting of the data  $a_{tf}^2 = 2.43 \times 10^{-24} M_\odot^{-1}$ . Accordingly the equation (5.9) reduces to

$$M_T = M_B + a_{tf} R_G M_B^{1/2}. \quad (5.22)$$

Using  $M_T$  as obtained from gravitational lensing observation of Abell 370 we can estimate  $M_B$  which turns out to be  $\sim 2 \times 10^{14}$  which is not consistent with the estimated baryonic mass of Abell 370 from photometric study. It seems that baryonic mass in baryonic Tully-Fisher relation should be replace by total mass that contains both luminous and dark matter mass.

## 5.4 Discussion and Conclusion

In this chapter the form of gravitational potential of galactic halo led by the flat rotation curve features is derived. The mass function is obtained considering the presence of cold dark matter in galaxy. The mass function will alter from that derived here if any other form of dark matter such as perfect fluid, or scalar field inspired dark matter state is considered. However, gravitational potential derived from lensing observations for a different choice of dark matter state instead of cold dark matter in general does not consistently match with that obtained from the flat rotation curve feature [228].

TABLE 5.2: Rotational velocity and baryonic mass data of different galaxies

Galaxy	$v(kms^{-1})$	$M_{stellar}(10^{10}M_{\odot})$	$M_{gas}(10^{10}M_{\odot})$
UGC 2885	300	30.8	5
NGC 2841	287	32.3	1.7
NGC 5533	250	19	3
NGC 6674	242	18	3.9
NGC 3992	242	15.3	0.92
NGC 7331	232	13.3	1.1
NGC 3953	223	7.9	0.27
NGC 5907	214	9.7	1.1
NGC 2998	213	8.3	3
NGC 801	208	10	2.9
NGC 5371	208	11.5	1
NGC 5033	195	8.8	0.93
NGC 3893	188	4.2	0.56
NGC 4157	185	4.83	0.79
NGC 2903	185	5.5	0.31
NGC 4217	178	4.25	0.25
NGC 4013	177	4.55	0.29
NGC 3521	175	6.5	0.63
NGC 4088	173	3.3	0.79
NGC 3877	167	3.35	0.14
NGC 4100	164	4.32	0.3
NGC 3949	164	1.39	0.33
NGC 3726	162	2.62	0.62
NGC 6946	160	2.7	2.7
NGC 4051	159	3.03	0.26
NGC 3198	156	2.3	0.63
NGC 2683	155	3.5	0.05
NGC 3917	135	1.4	0.18
NGC 4085	134	1	0.13
NGC 2403	134	1.1	0.47
NGC 3972	134	1	0.12
UGC 128	131	0.57	0.91
NGC 4010	128	0.86	0.27
F568-V1	124	0.66	0.34
NGC 3769	122	0.8	0.53
NGC 6503	121	0.83	0.24
F568-3	120	0.44	0.39
NGC 4183	112	0.59	0.34
F563-V2	111	0.55	0.32
F563-1	111	0.4	0.39
NGC 1003	110	0.3	0.82
UGC 6917	110	0.54	0.2
UGC 6930	110	0.42	0.31
M 33	107	0.48	0.13
UGC 6983	107	0.57	0.29
NGC 247	107	0.4	0.13
NGC 7793	100	0.41	0.1
NGC 300	90	0.22	0.13
NGC 5585	90	0.12	0.25
NGC 55	86	0.1	0.13
UGC 6667	86	0.25	0.08
UGC 2259	86	0.22	0.05
UGC 6446	82	0.12	0.3
UGC 6818	73	0.04	0.1
NGC 1560	72	0.034	0.098
IC 2574	66	0.01	0.067
DDO 170	64	0.024	0.061
NGC 3109	62	0.005	0.068
DDO 154	56	0.004	0.045
DDO 168	54	0.005	0.032

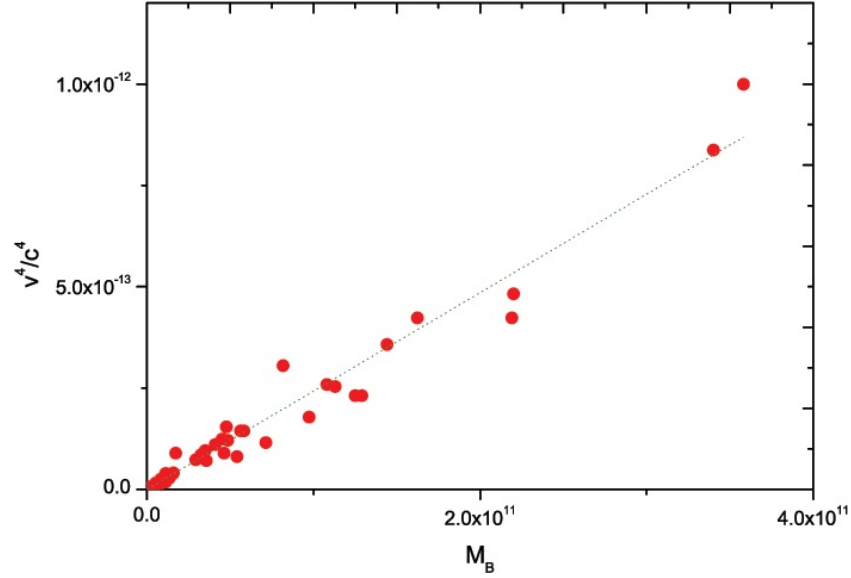


FIGURE 5.1: The variation of  $\beta_\varphi^4$  with  $M_B$  for several galaxies. The dotted line represents the least squared fit of the data.

Instead of exactly flat rotation curve i.e. instead of constant  $\beta_\varphi$  if we use universal halo velocity profile as given below [236, 237]

$$\beta_\varphi^2 = k \frac{r_a^2}{r_a^2 + r^2} \quad (5.23)$$

where  $\frac{\rho_o}{4\pi}$ ,  $\rho_o$  is the central density and  $r_a$  is a constant, the potential  $f(r)$  will become

$$f(r) \simeq k \ln[(r_a^2 + r^2)/R^2] \quad (5.24)$$

which reduces to Eq.(5.4) when  $r \gg r_a$ , with  $k = \beta_\varphi^2$ .

Numerical simulations suggest an approximate universality for the density profile of cold dark matter halos [238]. The density profile of dark matter prescribed by Navarro, Frenk and White (NFW) is widely used which is given by [238]

$$\rho(r) = \frac{\rho_s}{r/r_s(1 + r/r_s)^2} \quad (5.25)$$

The mass function corresponds to the NFW density profile will be

$$m_{NFW}(r) = 4\pi r_s^3 \rho_s \left( \frac{r_s}{r + r_s} + \text{Log}(r + r_s) \right) \quad (5.26)$$

However, for  $m_{NFW}(r)$  (together with  $\lambda$ ) the radial and transverse pressure of dark matter fluid do not vanish as expected for cold dark matter. The assumption of exactly flat rotation curve in deriving metric potential can be the reason for such an inconsistency.

The radial extension of a galaxy i.e. dark matter is so far not known which is one of the unanswered questions of modern astrophysics. Some alternative theories to GR, particularly conformal gravity can explain the galactic rotation curve without invoking any dark matter component [131]. However, the radial extent of galaxies in conformal theory [143] are not the same to the GR prediction and hence this feature is also a testable observable to differentiate the two models. In the present model the total mass of dark matter is proportional to the radius of galaxy. So if total mass is obtained say from lensing measurements and if baryonic mass is estimated from say photometric study, one can readily estimate the radial extension of a galaxy from equation (5.9) under the present framework and hence is an important testable parameter for the model.

In summary, we have derived gravitational field at halo of spiral galaxies in presence of cold dark matter considering observed flat rotation curve feature as an input. The gravitational lensing formulation have been derived for the halo metric. The lensing observation of Abell 370 is found to validate the derived halo space time. As a corollary the baryonic mass in baryonic Tully-Fisher relation seems to be replaced by total mass of a galaxy for consistent explanation of Abell 370 lensing observation.

In recent years few studies on dark matter distribution in galaxies have been made from lensing observations particularly using the Sloan Digital Sky Survey (SDSS) Data [239] and the Hubble Space Telescope observations [171]. However, the weak lensing signal in SDSS survey imaging is very noisy [154] and interpreted dark matter distribution in galaxies suffer from significant uncertainties. Future precise measurements of dark matter content within galactic halo independently from gravitational lensing and other methods should provide opportunity to further validate the derived halo metric.